



Research

# Alkali fusion of bauxite refining residue (red mud-RM) to produce low carbon cements



S. Pavia<sup>1</sup> · R. Goodhue<sup>2</sup> · O. Alelwee<sup>1</sup>

Received: 30 March 2023 / Accepted: 12 July 2023

Published online: 22 July 2023

© The Author(s) 2023 [OPEN](#)

## Abstract

This paper creates hydraulic binders using waste and a low energy input. Cements are produced with a bauxite refining residue (red mud-RM), blended with limestone and lime, and fused at temperatures from 600 to 1200 °C. The Saudi RM investigated has significant Al and Si but low Ca. Therefore, lime (CaO) and limestone (CaCO<sub>3</sub>) are used, as a source of calcium, to harvest cementing hydrates. When calcining RM alone, reactive aluminium phases begin to form at c.300 °C. However, at c.900 °C, they turn into crystalline corundum (Al<sub>2</sub>O<sub>3</sub>), a more stable and less reactive phase. It is hoped that the Ca provided by the lime/limestone will react with the Al in the RM during fusion, to form reactive silicates and aluminates rather than inert corundum. Both types of fusion produced calcium silicates and aluminates with cementing properties. However, lime fusion required higher temperature. Limestone fusion produces cementing phases at lower temperature than lime fusion, due to the lower decomposition temperature of CaCO<sub>3</sub> when compared to CaO. High temperature is required to break down CaO (melting point = 2572 °C), whereas CaCO<sub>3</sub> decomposes at 600 °C and disappears at 850 °C. Despite the top alkali fusion temperature being much lower than the CaO melting point, the results demonstrate that calcium was released from the lime and entered reactions forming calcium silicates and aluminates. This is probably due to the high alkali content of the RM acting as a flux and lowering the decomposition temperature of the CaO.

**Keywords** Bauxite refining residue · Red mud · Alkali fusion · Calcium silicates · Calcium aluminates · Gehlenite · Low-carbon cement

## 1 Introduction

Refining bauxite for the production of aluminium results in large volumes of red mud (RM) waste. Between 1 and 1.5 tons of RM waste are generated to obtain 1 ton of aluminium oxide [1]. 150 million tons of red mud are produced annually [2] and it is projected that 30 billion metric tons are accumulated in the world [3]. This paper studies the bauxite refining residue from the Ma'aden Mining Industries of Saudi Arabia which generate circa 6,000 tonnes of RM per day (over 2 Mt p.a.). This results in disposal problems and high land decommissioning costs

for landfill disposal. Therefore, to recycle this residue is of prime interest.

Portland cement (PC) has been the most important hydraulic binder for hundreds of years but is responsible for high environmental impact. PC clinker is made by heating, a mixture of natural rocks to a fusion temperature of about 1450 °C. This paper uses bauxite refining residue (RM) in lieu of non-renewable rocks and applies fusion temperatures ≤ 1200 °C to lower the energy input.

Due to its high alumina content, RM has been used in the cement and ceramic industries. It has been used to create ceramic material to manufacture bricks and insulations

✉ S. Pavia, [pavias@tcd.ie](mailto:pavias@tcd.ie) | <sup>1</sup>Department of Civil Engineering, University of Dublin, Trinity College, Dublin, Ireland. <sup>2</sup>Geochemistry Unit Department of Geology, University of Dublin, Trinity College, Dublin, Ireland.



[4]. It has also been used as an iron and Al source in PC production, whereby most iron and aluminium phases in the RM partake in the production of hydraulic  $C_3A$  and  $C_4AF$  [5]. Further applications of the bauxite refining residue include neutralisation of acidic soils, treatment of iron-deficient soils, and removal of toxic heavy metals from solutions [4]. Most RM residues are reactive, displaying pozzolanic properties. Alelwee et al. [6] state that the pozzolanic activity of RM is mainly due to the reaction of feldspathoids (cancrinite and sodalite) and the formation of zeolitic and feldspathoid-based hydrates. Previous authors increased the pozzolanic activity of the RM with heat treatments [7–9]. Alelwee et al. [6] studied the pozzolanic and cementing potential of the RM in this research. They conclude that the Saudi RM is moderately pozzolanic, and that thermal treatments enhance reactivity. Calcination at low temperatures of c.400 °C enhances the formation of pozzolanic hydrates that optimise setting and strength development.

RM usually contains significant Al and low Ca. The Si and Al can be active in an alkaline media. Therefore, RM has been activated with alkalis to produce alkali activated materials (AAMs) or geopolymers [10–13]. Geopolymers are a subset of AAMs with high Al and low Ca contents, therefore alkali-activated, RM materials are geopolymers. To produce geopolymers, RM is often activated with  $Na_2SiO_3$  and/or NaOH at varying ratios and concentrations. The alkalis are supposed to dissolve the minerals in the RM, breaking their bonds and liberating reactive monomers of Si and  $Al-[Si(OH)_4]^-$  and  $[Al(OH)_4]^-$  which form networks of repeating units by condensation, resulting in colloidal gels that provide strength [14, 15]. Alelwee and Pavia [16] made geopolymers with the RM in this study. They achieved significant strengths (~7 MPa) increasing to over 15 MPa when part of the RM was replaced with fly ash.

The Saudi RM investigated has significant Al and Si but low Ca. Therefore, lime (CaO) and limestone ( $CaCO_3$ ) are added, as a source of calcium, to harvest cementing hydrates. It is hoped that the calcium provided by the lime/limestone through alkali fusion, will participate in reactions so that the Al in the RM forms reactive silicates and aluminates rather than inert corundum.

In summary, RM waste has been used to produce geopolymers and ceramic materials, and applied to soil for neutralisation and iron-deficiency. As aforementioned, several authors have demonstrated that RM is pozzolanic and hence it can be used as a supplementary cementitious material in PC production. However, no studies to date have attempted to produce a hydraulic cement using RM. This paper attempts to create a hydraulic cement using RM waste blended with limestone and lime and fused at temperatures ranging from 600 to 1200 °C.

No measurement of carbon content is provided in this paper. However, the main component of the cements investigated is red mud waste which amounts to 65% wt. Red mud is generated as a waste during the refining of bauxite to produce aluminium. As a by-product, the energy and carbon emissions from its manufacturing are zero. So, the main carbon input in the cements investigated are due to the quarrying of the limestone or the lime production, and the decarbonation of the materials during fusion. The limestone/lime amounts 35% wt in the cements investigated. Therefore, their carbon contribution is much lower than that of traditional PC production where over 95% of the raw materials are carbon sources. The energy input for calcination is also lower than traditional cement production at 600–1200 °C.

## 2 Materials and methods

Bauxite refining waste (RM) from the Ma'aden Mining Industries is studied. The refining temperatures range between 260 and 270 °C, and quick lime is added twice during the refining process (Abdul Malik Shaheen, pers. Com. Ma'adem 2020). The RM consists of gibbsite and boehmite, inherited from the parent bauxite, and cancrinite, chantalite and sodalite formed during the Bayer process. The CaO, added during refining, has transformed the original goethite into hematite, and caused the occurrence of cancrinite [6]. The location of the Az Zabirah mine which is the RM source is included in Fig. 1 [17].

The RM was blended with lime and limestone at temperatures ranging from 600–1200 °C for three hours. The lime is a pure calcium lime, in quick lime form, complying with European standards (designation CL90Q). The limestone is a Portland limestone from the UK, consisting of calcite ( $CaCO_3$ ), with traces of silica in the form of quartz ( $SiO_2$ ) (Table 1). It comprises abundant microcrystalline  $CaCO_3$  (micrite), with a higher specific surface and a greater reactivity than coarser, more crystalline carbonate grains [18, 19]. The limestone and RM were ground to reach a specific surface area of 3.29 m<sup>2</sup>/g and 9.35 m<sup>2</sup>/g respectively to increase the specific surface area available for reaction. The process of calcining the lime/limestone and RM at high temperature is known as alkali fusion. Alkali fusion can convert low-reactivity crystalline wastes into reactive materials. Mao et al. [20] report that fusing basalt with NaOH increased reactivity by approximately 30%. According to Liu et al. [21] crystalline minerals in mine tailings turned into amorphous reactive sodium aluminosilicate after alkali fusion.

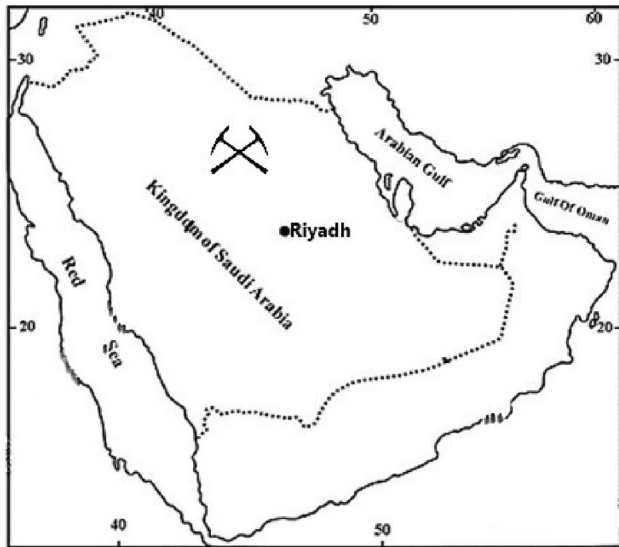


**Fig. 1** Location of the Az Zabirah mine (bauxite refining residue source) by Al-Mutari, Galmed and Aldamegh [17]. Reproduced with the authors' permission

### 2.1 Mix design. Calculation of the quantity of CaO and limestone ( $\text{CaCO}_3$ ) to be added to the bauxite refining residue.

The blending quantity of lime/limestone was fixed at 35% wt. This was determined based on the ratio of CaO to  $\text{SiO}_2$  in PC production which shall be not be less than 2.0. The red mud residue includes approximately 20% silica and < 5% CaO -Table 2. The standard deviation of the XRF results for 2 samples taken 12 months apart is < 2 in all measurements. Therefore, the cements were blended to include 65% RM: 35% CaO and 65% RM: 35%  $\text{CaCO}_3$  (~ 2: 1 by weight).

The mixes were sintered at temperature ranging from 600 to 1200 °C for 3 h. Subsequently, pastes were produced with the cements and varying water content (Table 3). The water content slightly varied because it was determined to make the cements flow to a workable

**Table 3** Water content required for the cement pastes (RM:  $\text{CaO}/\text{CaCO}_3 \sim 2: 1$  by weight) to reach an initial flow diameter of 170–175 mm.  $b^* = \text{RM} + \text{CaO}/\text{CaCO}_3$

Cement components and fusing $T^\circ\text{C}$	w/b*
RM + limestone 600	0.65
RM + limestone 800	0.71
RM + limestone 1000	0.89
RM + limestone 1200	0.94
RM + CaO 600	1.05
RM + CaO 800	1.05
RM + CaO 1000	0.80
RM + CaO 1200	0.80
CaO	1.80
Limestone	0.75

consistency, an initial flow diameter ranging from 170 to 175 mm.

### 2.2 Characterization of the resultant cements

The mineral composition of the cements sintered was studied with X-Ray diffraction (XRD). A Phillips PW1720 XRD system was used, with a PW1050/80 goniometer and a PW3313/20 Cu k-alpha anode tube at 40 kV and 20 mA. The diffraction angles were recorded between 3 and 60 degrees ( $2\theta$ ) at a step size of 0.02 degrees/second. The microstructure and the nature of the hydrates formed by the sintered cements in the pastes above (Table 3) were studied with a scanning electron microscope (SEM) and an energy dispersive X-Ray analysis attachment (EDXRA). The EDXRA allowed investigating the elemental composition of the hydrates.

## 3 Results

### 3.1 Characterisation of the bauxite residue

The red mud was studied by Alelweet et al. [6]. As noted by the authors, the residue has high silica and

**Table 1** Composition (% by mass, X-Ray Fluorescence analyses) of the Portland limestone base bed [18, 19]

Ca $\text{CO}_3$	Mg carbonates	$\text{Al}_2\text{O}_3$	$\text{Fe}_2\text{O}_3$	$\text{SiO}_2$	Water/other	Porosity %
95.8	1.2	0.3	0.3	1.3	1.4	15.4

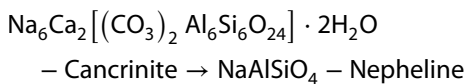
**Table 2** Chemical composition of the red mud as a % by wt oxide in [6]

Red Mud**	$\text{SiO}_2$	$\text{Al}_2\text{O}_3$	CaO	$\text{Fe}_2\text{O}_3$	$\text{Na}_2\text{O}$	K <sub>2</sub> O	MgO	$\text{P}_2\text{O}_5$	$\text{SO}_3$	Cl	$\text{TiO}_2$	MnO	CuO	SrO	$\text{ZrO}_2$
	19.66	29.79	5.09	12.97	24.05	0.09	0.40	0.29	1.65	0.32	5.12	0.02	0.00	0.14	-

\*\*Traces of  $\text{V}_2\text{O}_5 = 0.138\%$ ;  $\text{Cr}_2\text{O}_3 = 0.074\%$ ;  $\text{NiO} = 0.003\%$ ;  $\text{ZnO} = 0.002\%$ ;  $\text{Ga}_2\text{O}_3 = 0.005\%$ ;  $\text{As}_2\text{O}_3 = 0.005\%$ ;  $\text{Y}_2\text{O}_3 = 0.006\%$

alumina contents (Table 2). The levels of arsenic and chromium or any heavy metals are low, and hence no environmental toxicity is evident. The major mineral phases in the RM are hematite-Fe<sub>2</sub>O<sub>3</sub>, cancrinite -Na<sub>6</sub>Ca<sub>2</sub>[(CO<sub>3</sub>)<sub>2</sub>Al<sub>6</sub>Si<sub>6</sub>O<sub>24</sub>]·2H<sub>2</sub>O-, gibbsite -Al (OH)<sub>3</sub> and sodalite -Na<sub>4</sub> Si<sub>3</sub>Al<sub>3</sub> O<sub>12</sub>Cl- (Fig. 2 and Table 4). As aforementioned, the NaOH and lime used during the bauxite refining process react with the kaolinite in the parent bauxite forming the feldspathoids cancrinite and sodalite [6].

reactive phases with cementing potential. First, gibbsite dehydroxylates (at 300 °C) transforming into boehmite- γ-AlO(OH), and likely amorphous alumina polymorphs [6]. Hence providing active Al<sup>3+</sup> and OH<sup>-</sup>. Later, at 1000 °C, the feldspathoids (cancrinite, sodalite) transform into nepheline (Na Al SiO<sub>4</sub>), tri-calcium aluminate (C<sub>3</sub>A-Ca<sub>3</sub>Al<sub>2</sub>O<sub>4</sub>) and gehlenite (Ca<sub>2</sub>Al<sub>2</sub>SiO<sub>7</sub>) - Table 5.



### 3.2 Characterization of the resultant cements

When calcining red mud alone, there are two main transformations that provide ions and radicals which can produce

Fig. 2 Mineral assemblage of the bauxite residue, red mud

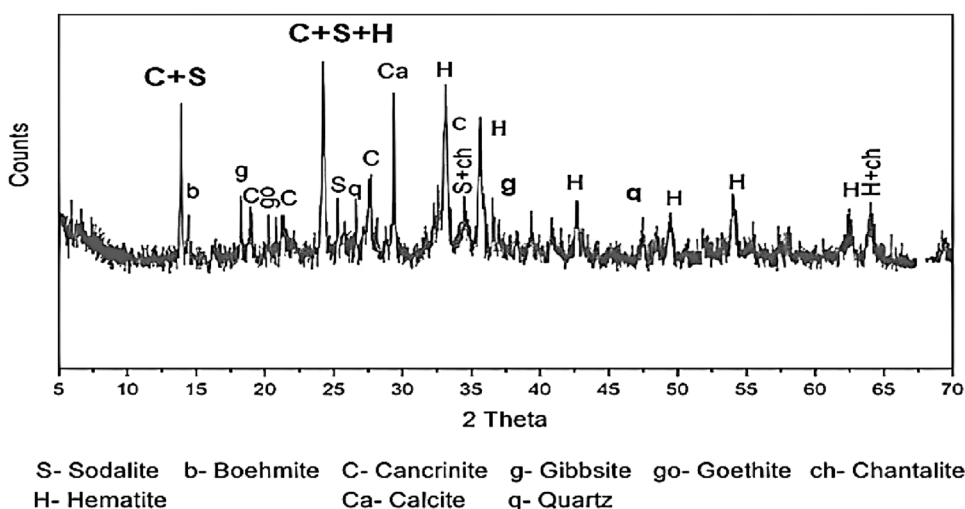
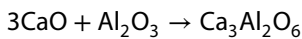


Table 4 Mineral composition of the RM residue determined with XRD [6]

Mineral composition by XRD		
<i>RM</i>		
Major phases (40 – 15%)	Subsidiary (15 – 7%)	Traces < 7%
Hematite -Fe <sub>2</sub> O <sub>3</sub>	Boehmite- γ- AlO(OH)	Quartz SiO <sub>2</sub>
Cancrinite -Na <sub>6</sub> Ca <sub>2</sub> [(CO <sub>3</sub> ) <sub>2</sub> Al <sub>6</sub> Si <sub>6</sub> O <sub>24</sub> ]·2H <sub>2</sub> O	Calcite CaCO <sub>3</sub>	Rutile TiO <sub>2</sub>
Gibbsite -Al (OH) <sub>3</sub>		Goethite α-FeOOH
Sodalite -Na <sub>4</sub> Si <sub>3</sub> Al <sub>3</sub> O <sub>12</sub> Cl		Chantalite—CaAl <sub>2</sub> (SiO <sub>4</sub> )(OH) <sub>4</sub>

Table 5 Evolution of the mineral assemblage of the RM with increasing temperature determined with XRD. XX-Abundant (~ 40%); X-subsidiary (40 – 15%); (X)-minor (15 – < 7%). Green arrows mark transformations

T°C	Hematite Fe <sub>2</sub> O <sub>3</sub>	Cancrinite Na <sub>6</sub> Ca <sub>2</sub> [(CO <sub>3</sub> ) <sub>2</sub> Al <sub>6</sub> Si <sub>6</sub> O <sub>24</sub> ]·2H <sub>2</sub> O	Sodalite Na <sub>4</sub> Si <sub>3</sub> Al <sub>3</sub> O <sub>12</sub> Cl	Gibbsite Al (OH) <sub>3</sub>	Boehm γ AlO(OH)	Chantalite CaAl <sub>2</sub> (SiO <sub>4</sub> )(OH) <sub>4</sub>	Nepheline Na Al SiO <sub>4</sub>	Gehlenite Ca <sub>2</sub> Al <sub>2</sub> SiO <sub>7</sub>	C <sub>3</sub> A Ca <sub>3</sub> Al <sub>2</sub> O <sub>6</sub>
0	XX	X	X	X		(X)			
300	XX	X	X		X	(X)			
400	XX	X(X)	X		X	(X)			
750	XX	X	X			(X)			
1000	XX		(X)				X	(X)	(X)



– tricalcium aluminate (or  $3\text{CaO} \cdot \text{Al}_2\text{O}_3$ )

Therefore, when calcining RM alone, at  $\sim 1000^\circ\text{C}$ , the formation of nepheline from cancrinite releases CaO which is involved in the formation of tricalcium aluminate  $-\text{Ca}_3\text{Al}_2\text{O}_6$  [8]. RM is low in calcium (Table 2). Therefore, it was planned that the additional  $\text{Ca}^{2+}$  provided by the limestone/lime during alkali fusion would enhance the formation of calcium aluminates and calcium aluminosilicates (CAS) in the new cements. It was also projected that reactions leading to the formation of active phases would take place at lower temperatures, as  $\text{Al}^{3+}$  and amorphous alumina hydrates are available as early as  $300^\circ\text{C}$  and limestone ( $\text{CaCO}_3$ ) begins to decompose at  $650^\circ\text{C}$ .

### 3.2.1 Alkali fusion with lime (CaO)

As projected, the additional  $\text{Ca}^{2+}$  provided by the lime has enabled the formation of more abundant reactive phases, and they appear at a slightly lower temperature than when burning the RM alone (there are traces of reactive phases at  $800^\circ\text{C}$ —Fig. 3). As the fusion temperature increases, calcium silicates and calcium aluminates begin to appear. Significant amounts of reactive silicates  $\text{C}_2\text{AS}$ —gehlenite- and  $\text{C}_3\text{A}$  -tricalcium aluminate- appear at  $1000^\circ\text{C}$  and above (Fig. 3). The XRD trace of the cement, made with the RM fused with lime at  $1000^\circ\text{C}$ , revealed the presence of portlandite  $-\text{Ca}(\text{OH})_2$ —and calcium olivine  $-\text{Ca}_2\text{SiO}_4$  (Fig. 4). Increasing the temperature further to  $1200^\circ\text{C}$  (Fig. 5) produces larnite ( $\text{Ca}_2\text{SiO}_4$ ) and perovskite ( $\text{CaTiO}_3$ ).

CaO has a high melting point of  $2572^\circ\text{C}$ , but the fusion temperature used in this research only reached  $1200^\circ\text{C}$  to keep energy input as low as possible. However, despite the CaO melting point being much greater than the fusion temperature, it is evident from the presence of calcium silicates and calcium aluminates (Figs. 3, 4, 5), that the calcium in the lime has entered in reactions during fusion. This is probably due to the high alkali content in the red mud residue which has acted as a flux, lowering the decomposition temperature of the CaO.

A flux is a material that lowers the melting temperature of a mix and increases the amount of melt produced at a given temperature. For example, in PC production, the clinkering temperature must be reached for the raw materials to fuse and calcium silicates and aluminates (PC clinkers) to form. The temperature above which liquid forms is  $1338^\circ\text{C}$ , but minor components act as fluxes lower this temperature [22]. Although fluxes normally decrease melting temperatures only slightly, they rise the amount of liquid produced at a certain temperature. The liquid is the medium in which the reactants move to form hydraulic clinkers, the greater the amount of liquid, the more reactants are carried, and hence more abundant clinkers are formed.  $\text{MgO}$ ,  $\text{Al}_2\text{O}_3$ ,  $\text{Fe}_2\text{O}_3$ , alkalis, lime, fluor compounds and sulphates can act as a flux [23].

As aforementioned, pastes were fabricated using the cements sintered by alkali fusion, and the nature of the cementing hydrates in the pastes was investigated with a SEM/EDX system. The general appearance of the hydrates which formed in the cements fabricated by fusing the bauxite residue with lime at  $1200^\circ\text{C}$  is shown in Fig. 6. The SEM evidenced low-crystallinity gels with the morphology

**Fig. 3** Mineral transformation of RM fused with CaO at increasing temperature. CH- Portlandite-  $\text{Ca}(\text{OH})_2$ ; OL- olivine  $-\text{Ca}_2\text{SiO}_4$ ; L- Larnite— $\text{Ca}_2\text{SiO}_4$ ;  $\text{C}_2\text{AS}$ - gehlenite;  $\text{C}_3\text{A}$ -tricalcium aluminate

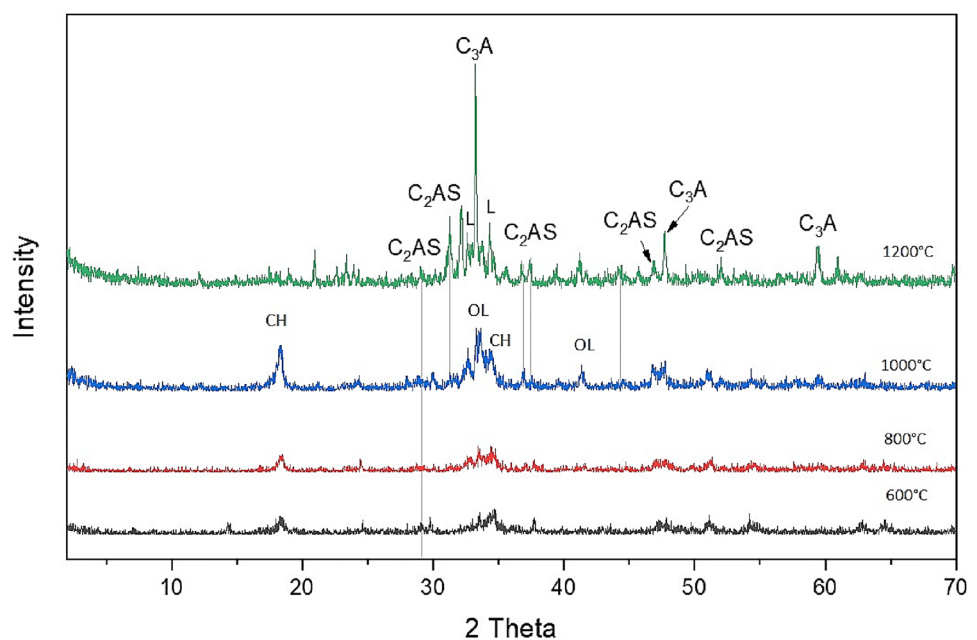


**Fig. 4** Detail of the mineral composition of the RM fused with CaO at 1000 °C

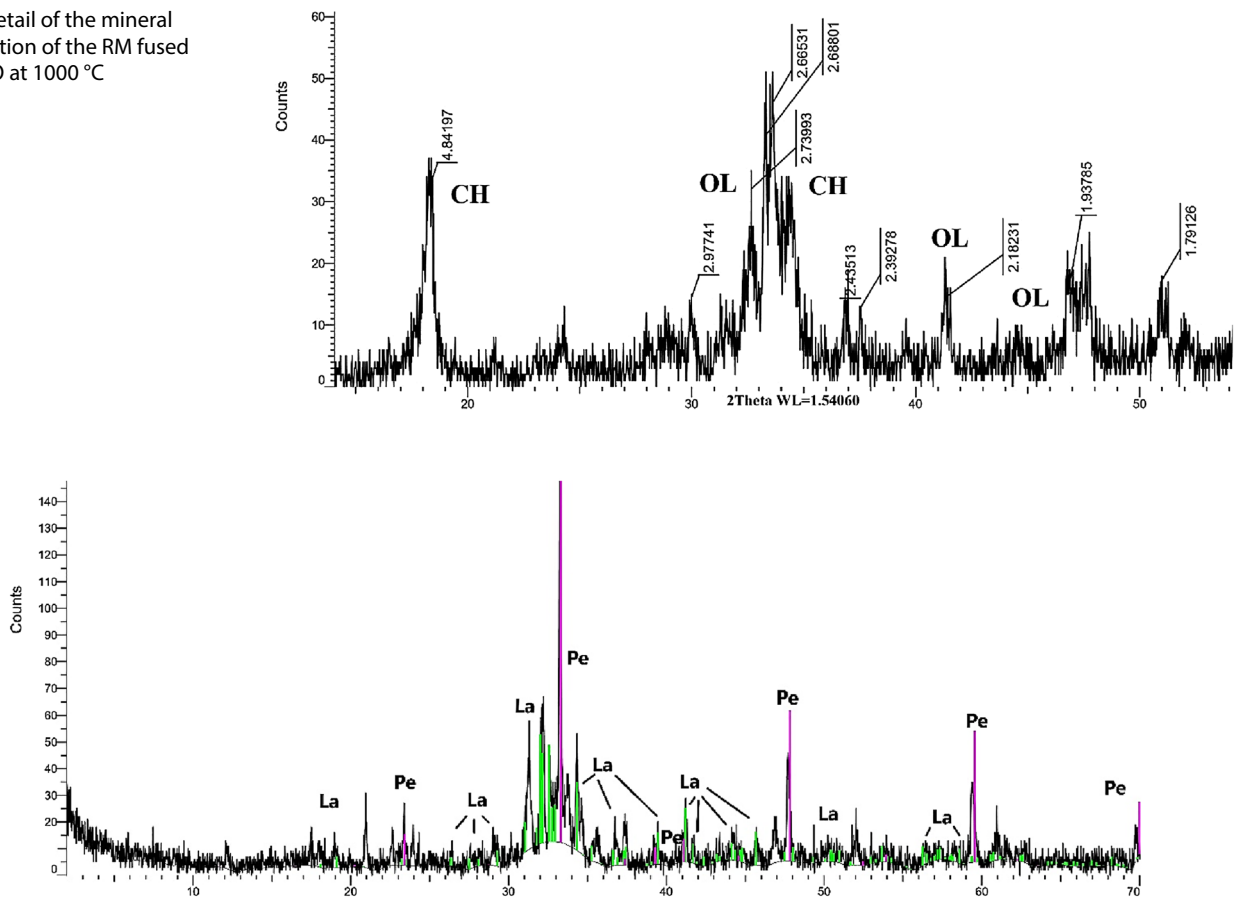


**Fig. 5** Detail of the mineral composition of the RM fused with CaO at 1200 °C including larnite  $\text{-Ca}_2\text{SiO}_4\text{-}$  marked as La in green, and  $\text{C}_3\text{A}$ /perovskite (Pe-purple)  $\text{-CaTiO}_3$

typical of C–S–H and plate-like phases with the typical appearance of AFm phases. Their EDX spectrums show varying contents of Si, Al and Ca, and occasionally high Na content (Fig. 6). The hydration of  $\text{C}_2\text{AS}$ – gehlenite and  $\text{C}_3\text{A}$ –tricalcium aluminate can provide such cementing hydrates. Doval et al. [24] report that when gehlenite  $\text{-C}_2\text{AS-}$  hydrates it forms plate crystal of gehlenite hydrate incorporated into a groundmass of fine C–S–H crystals.

### 3.2.2 Alkali fusion with limestone ( $\text{CaCO}_3$ )

Fusing the bauxite residue with limestone produces more abundant reactive silicates and aluminates than lime fusion (Fig. 7). Abundant calcium silicates and fewer calcium aluminates were recorded with XRD including gehlenite  $\text{-C}_2\text{AS-}$ ; calcium aluminates  $\text{C}_{12}\text{A}_7$  and  $\text{C}_2\text{A}$ , sodium calcium silicate and sodium aluminium silicate. Silicates (gehlenite -calcium aluminium silicate  $\text{-C}_2\text{AS-}$  and sodium aluminium silicate), have formed in the cement, even at the lowest fusion temperature of 600 °C—Fig. 7. The abundance, varied nature, and early appearance of the

reactive phases in the cement is due to the low decomposition temperature of  $\text{CaCO}_3$  which begins to decompose at 600 °C and disappears at 850 °C. The results in Fig. 7 prove that, at 600 °C, some limestone has already decomposed, providing  $\text{Ca}^{2+}$  that has entered fusion reactions to form gehlenite  $\text{-C}_2\text{AS-}$ .

The general appearance of the hydrates formed in the cements obtained when fusing the bauxite residue with limestone at 800 and 1200 °C is shown in Figs. 8 and 9 respectively. Similarly to the lime-fused cement hydrates, the SEM evidenced low-crystallinity gels with the typical morphology of C–S–H and plate-like phases with the typical appearance of AFm phases. Their morphology and EDX spectrums are inconclusive (Figs. 8, 9).

## 4 Conclusion

Hydraulic cements are produced, with a relatively low energy input, using refining bauxite waste (RM). The RM is high in Al and Si but low in Ca, therefore it is blended

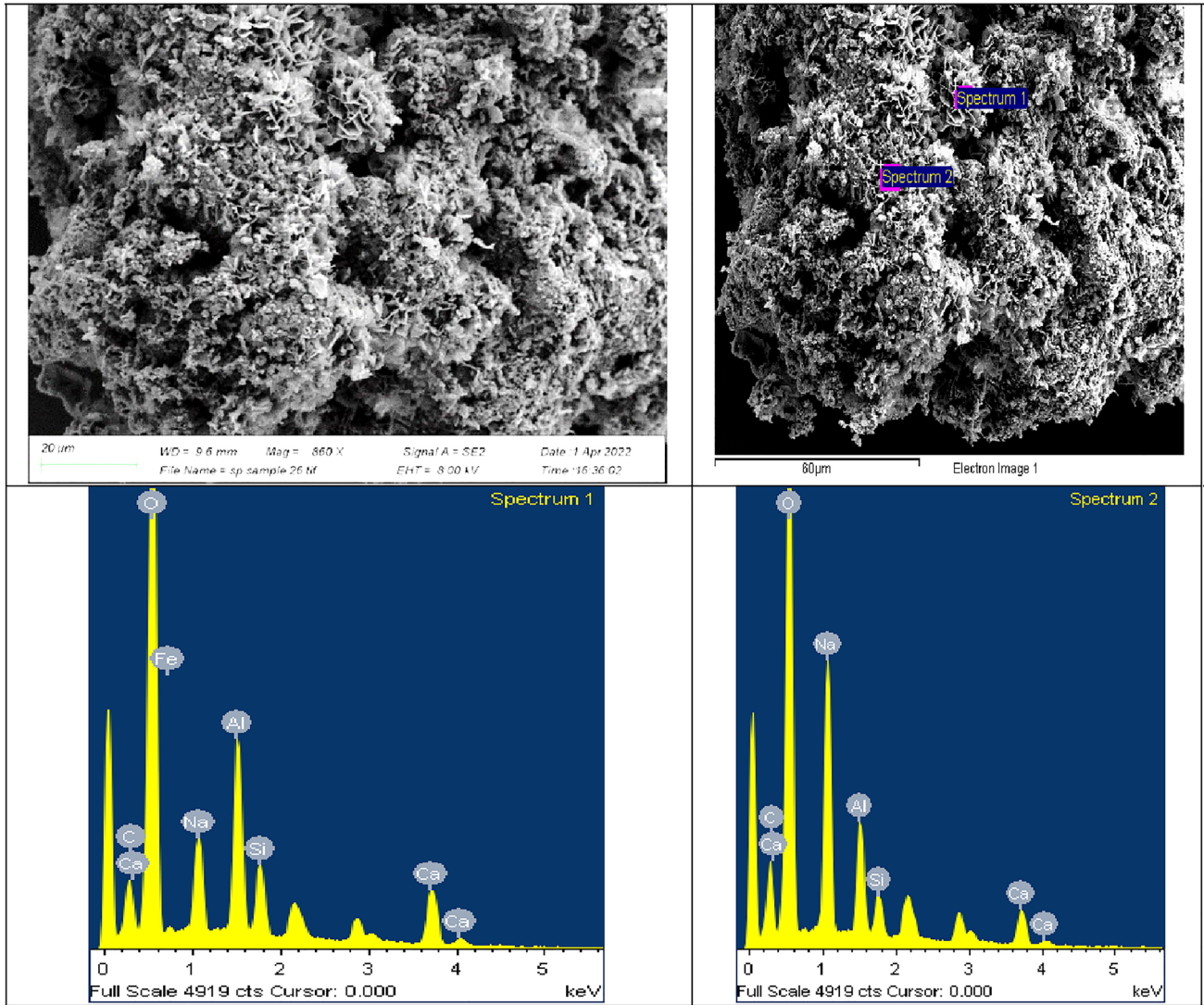
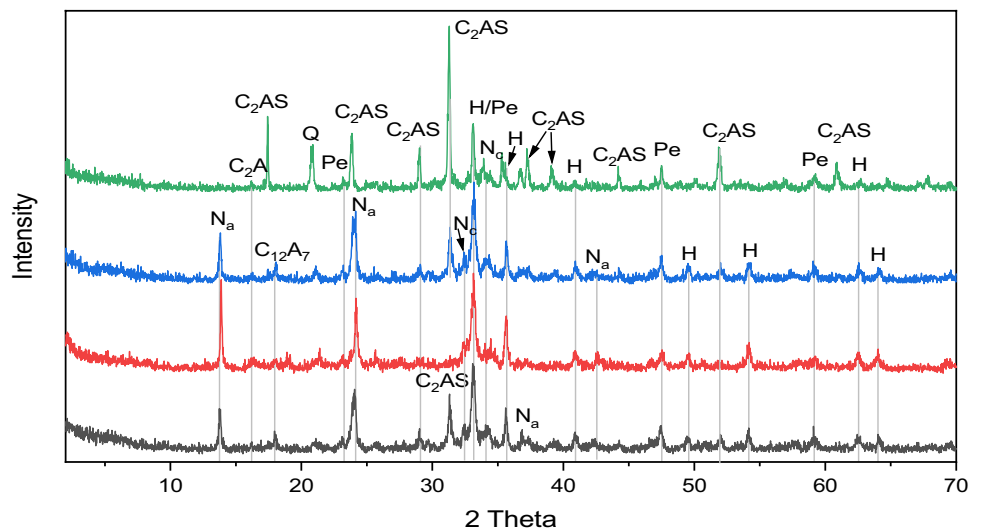
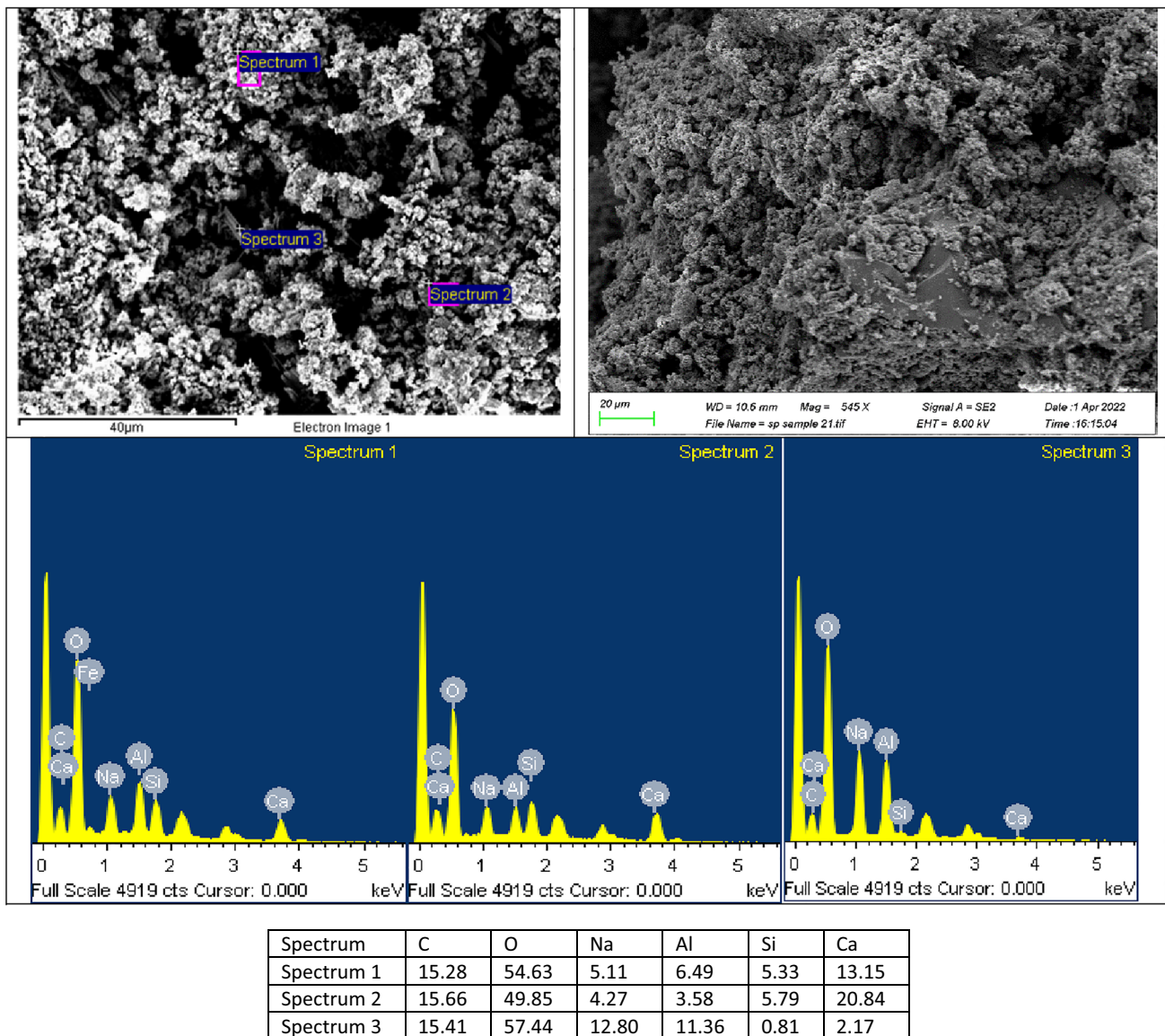


Fig. 6 Representative SEM images and elemental analyses of the hydrates formed in the paste made with RM: CaO cement fused at 1200 °C

Fig. 7 Mineral transformation of RM fused with limestone at increasing temperature. From top to bottom: Green 1200 °C; Blue 1000 °C; Red 800 °C; Black 600 °C. Q-quartz-SiO<sub>2</sub>; Pe- Perovskite-CaTiO<sub>3</sub>; H- hematite-Fe<sub>2</sub>O<sub>3</sub>; Nc – sodium calcium silicate; Na – sodium aluminium silicate





**Fig. 8** Representative SEM images and elemental analyses of the hydrates formed in the paste made with RM: limestone cement fused at 800 °C

with limestone or lime, as a source for  $Ca^{2+}$ , and fused at temperatures from 600 to 1200 °C.

Both lime and limestone fusion produced calcium silicates and aluminates with cementing properties. They reduced the sintering temperature, and increased the amount of reactive phases produced when compared to the calcination of RM alone. Even at low temperature (600 °C), the  $Ca^{2+}$  provided by the lime/limestone participates in reactions and combines with the  $Al^{3+}$  in RM to form reactive silicates and aluminates with cementing properties.

Lime fusion required higher temperature than limestone fusion to provide reactive phases with cementing properties. This is due to the high temperature required to

break down  $CaO$ , with a melting point of 2572 °C. Despite the top fusion temperature (1200 °C) being much lower than the lime’s melting point (2572 °C), calcium released from the lime entered reactions and formed calcium silicates and aluminates. This is probably due to the high alkali content in the RM acting as a flux, lowering the decomposition temperature of the lime.

Limestone fusion produces cementing phases at much lower temperature than lime fusion, because  $CaCO_3$  begins to decompose at low temperature (600 °C) and disappears at 850 °C. Reactive phases (gehlenite  $-C_2AS-$  and sodium aluminium silicate) appear in the cements at 600 °C. Limestone fusion produces more abundant reactive phases, more varied in composition, including gehlenite  $-C_2AS-$ ;



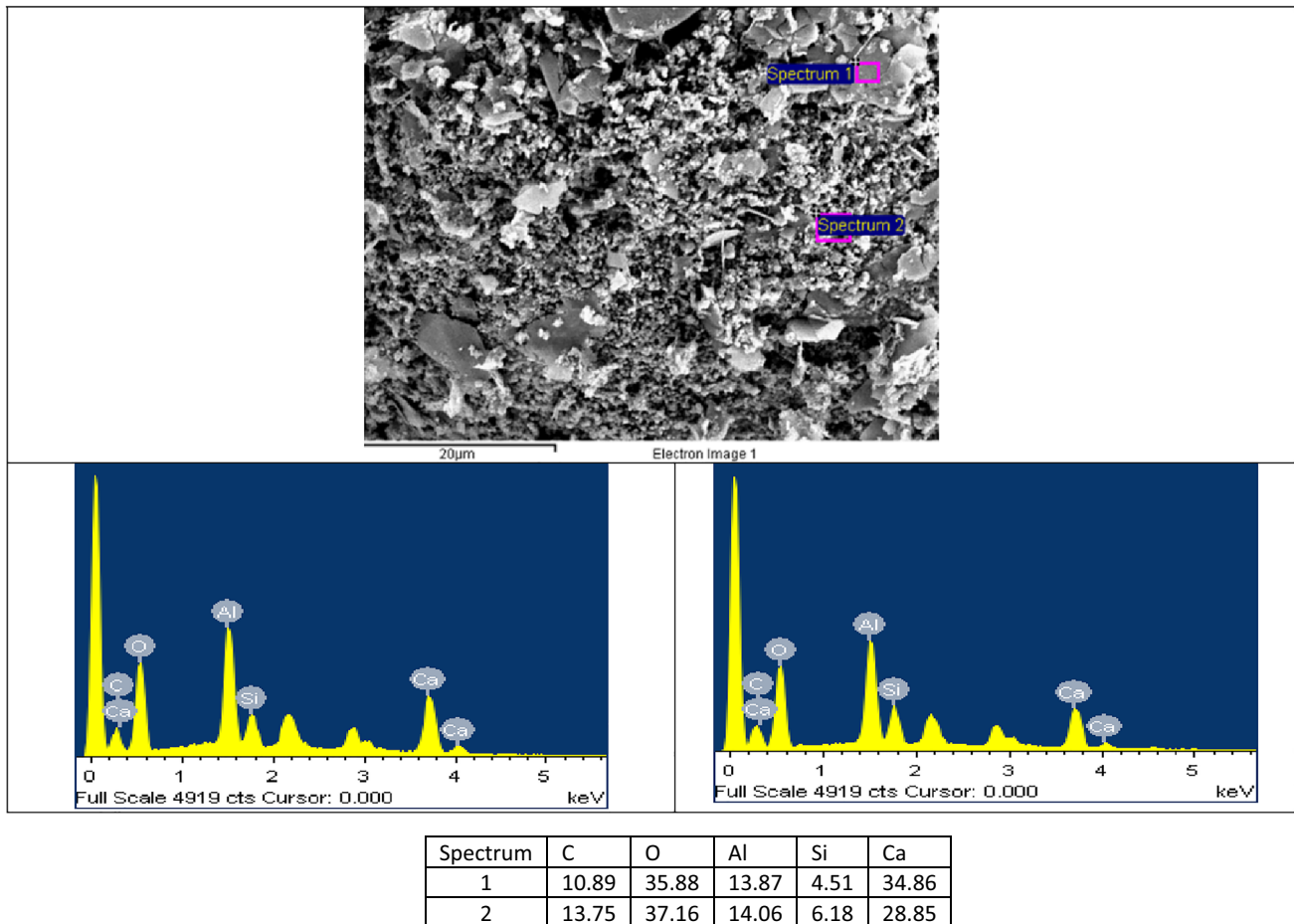


**Fig. 9** Representative SEM images and elemental analyses of the hydrates formed in the paste made with a RM: limestone cement fused at 1200 °C. Left: spectrum 1; Right spectrum 2

calcium aluminates  $C_{12}A_7$  and  $C_2A$ , sodium calcium silicate and sodium aluminium silicate. Further work is needed to determine with more detail the mineralogy of the cementing hydrates, and the strength afforded by the hydration of the calcium silicates and aluminates comprising the cements.

**Acknowledgements** The authors thank Abdul Malik Shaheen of Ma'adem for providing valuable information of the processing and refining process of the bauxite ore in the Ma'adem refineries. The authors also thank the Government of Saudi Arabia, Technical & Vocational Training Corporation and the Saudi Arabian Cultural Bureau for their support and for financing the project. We thank Dr J. Canavan, Geography Department, TCD, and D. Daly of AMBER, the SFI Research Centre for Advanced Materials and BioEngineering Research and CRANN Institute, TCD, for their assistance with the analyses.

**Author contributions** S.P.—Conception, manuscript composition. R.G.—Experimental work. O.A.—PhD research background and laboratory work.

**Data availability** The datasets generated during and/or analysed during the current study are available from the corresponding author on reasonable request.

## Declarations

**Competing interests** The authors declare no competing interests.

**Open Access** This article is licensed under a Creative Commons Attribution 4.0 International License, which permits use, sharing, adaptation, distribution and reproduction in any medium or format, as long as you give appropriate credit to the original author(s) and the source, provide a link to the Creative Commons licence, and indicate if changes were made. The images or other third party material in this article are included in the article's Creative Commons licence, unless indicated otherwise in a credit line to the material. If material is not included in the article's Creative Commons licence and your intended use is not permitted by statutory regulation or exceeds the permitted use, you will need to obtain permission directly from the copyright holder. To view a copy of this licence, visit <http://creativecommons.org/licenses/by/4.0/>.

## References

1. Khairul MA, Zanganeh J, Moghtaderi B (2019) The composition, recycling and utilisation of Bayer red mud. *Res Cons Recycl* 141:483–498. <https://doi.org/10.1016/j.resconrec.2018.11.006>
2. Kumar S, Kumar R, Bandopadhyay A (2006) Innovative methodologies for the utilisation of wastes from metallurgical and allied industries. *Res Cons Recycl* 48(4):301–314
3. Mishra B, Gostu S (2017) Materials sustainability for environment: red-mud treatment. *Front Chem Sci Eng* 11(3):483–496. <https://doi.org/10.1007/s11705-017-1653-z>
4. Hind AR, Bhargava SK, Grocott SC (1999) The surface chemistry of Bayer process solids: a review. *Colloids Surf A Physicochem Eng Aspects* 146(1–3):359–374. [https://doi.org/10.1016/S0927-7757\(98\)00798-5](https://doi.org/10.1016/S0927-7757(98)00798-5)
5. Pontikes Y, Angelopoulos GN (2013) Bauxite residue in cement and cementitious applications: current status and a possible way forward. *Res, Cons Recycl* 73:53–63. <https://doi.org/10.1016/j.resconrec.2013.01.005>
6. Alelweet O, Pavia S, Lei Z (2021) Pozzolanic and cementing activity of raw and pyro-processed Saudi Arabian red mud (RM) waste. *Recent Progr Mat* 3(4):139–164. <https://doi.org/10.21926/rpm.2104047>
7. Pera J, Boumaza R, Ambrose J (1997) Development of a pozzolanic pigment from red mud. *Cem Concr Res* 27(15):13–22
8. Sglavo VM, Campostrini R, Maurina S, Carturan G, Monagheddu M, Budroni G, Cocco G (2000) Bauxite ‘red mud’ in the ceramic industry. Part 1: thermal behavior. *J Eur Ceram Soc* 20:235–244
9. Manfroï EP, Cheriaf M, Cavalcante Rocha J (2014) Microstructure, mineralogy and environmental evaluation of cementitious composites produced with red mud waste. *Cons Build Mat Part A* 67:29–3. <https://doi.org/10.1016/j.conbuildmat.2013.10.031>
10. Kumar A, Kumar S (2013) Development of paving blocks from synergistic use of red mud and fly ash using geopolymerization. *Cons Build Mat* 38:865–871. <https://doi.org/10.1016/j.conbuildmat.2012.09.013>
11. Hajjaji W, Andrejkovičová S, Zanelli C, Alshaaer M, Dondi M, Labrincha JA, Rocha F (2013) Composition and technological properties of geopolymers based on metakaolin and red mud. *Mat Design* 1980–2015(52):648–654
12. Singh S, Biswas R, Das MU, Aswath MU (2016) Experimental study on red mud based geopolymer concrete with fly ash & GGBS in ambient temperature curing. *Int. J. Adv. Mech. Civ. Eng.* ISSN 3:2394–2827
13. Singh S, Aswath MU, Ranganath RV (2018) Effect of mechanical activation of red mud on the strength of geopolymer binder. *Cons Build Mat* 177:91–101. <https://doi.org/10.1016/j.conbuildmat.2018.05.096>
14. Davidovits J (1994) Properties of geopolymer cements. *First Int Conf Alkaline Cem Concr* 1:131–149
15. Duxson PSWM, Mallicoat SW, Lukey GC, Kriven WM, Van Deventer JS (2007) The effect of alkali and Si/Al ratio on the development of mechanical properties of metakaolin-based geopolymers. *Colloids Surf A Phys Eng Asp* 292(1):8–20. <https://doi.org/10.1016/j.colsurfa.2006.05.044>
16. Alelweet O, Pavia S (2023) Properties of alkali activated materials made with bauxite refining residue (red mud-RM) and blends of RM with fly ash (FA). *CEES 2023 2<sup>nd</sup> Int. Conf. on construction, energy, environment & sustainability*, Funchal. Portugal. Ed. by ITECONS. ISBN: 978-989-54499-3-4
17. Al-Mutairi MA, Galmed KS, Aldamegh AN (2015) Petrogenesis of the Az Zabirah south zone bauxite ore deposits, central northern Saudi Arabia Arabia. *J Geosci* 8:2327–2339. <https://doi.org/10.1007/s12517-014-1347-5>
18. Pavia S, Aly M (2016) Influence of aggregate and supplementary cementitious materials on the properties of hydrated lime (CL90s) mortars. *Mater Constr* 66(324):e104. <https://doi.org/10.3989/mc.2016.01716>
19. Pavia S, Aly M (2019) Sustainable, hydraulic-lime-limestone binders for construction. *Adv Civ Eng Mater* 8(3):235–254. <https://doi.org/10.1520/ACEM20180124>
20. Mao Q, Li Y, Liu K, Peng H, Shi X (2022) Mechanism, characterization and factors of reaction between basalt and alkali: exploratory investigation for potential application in geopolymer concrete. *Cem Concr Comp* 130:104526. <https://doi.org/10.1016/j.cemconcomp.2022.104526>
21. Liu Q, Cui M, Li X, Wang J, Wang Z, Li L, Lyu X (2022) Alkali-hydrothermal activation of mine tailings to prepare one-part geopolymer: activation mechanism, workability, strength, and hydration reaction. *Cer Int* 48(20):318. <https://doi.org/10.1016/j.ceramint.2022.06.318>
22. Harrison AM (2019) Constitution and specification of portland cement. In: Hewlett PC, Liska M (eds) *Lea’s chemistry of cement and concrete* (5th Edn). Elsevier, Netherlands
23. Hewlett PC, Liska M (eds) (2019) *Lea’s chemistry of cement and concrete*, 5th edn. Elsevier, Netherlands
24. Dováł M, Palou M, Mojumdar SC (2006) Hydration behavior of C<sub>2</sub>S and C<sub>2</sub>AS nanomaterials, synthesized by sol–gel method. *J Therm Anal Calorim* 86:595–599. <https://doi.org/10.1007/s10973-006-7713-0>

**Publisher’s Note** Springer Nature remains neutral with regard to jurisdictional claims in published maps and institutional affiliations.